of pyrene groups. A very strong hypochromic effect suggests that in these species the pyrenes are stacked face-to-face.

Acknowledgment. We thank Dr. T. Ikeda and Mr. Y. Kawanishi (Tokyo Institute of Technology) for fluorescence decay measurements. F.M.W. thanks Xerox Corp. for permission for her extended stay in Tokyo. M.A.W. thanks the Japan Society for the Promotion of Science for a fellowship.

Registry No. HPC, 9004-64-2; H_2O, 7732-18-5; MeOH, 67-56-1; $MeCH_2OH$, 64-17-5; $MeCH_2OCH_2CH_2OH$, 110-80-5; $HO(CH_2)_2O(CH_2)_2OH$, 111-46-6; $HOCH_2CH(OH)CH_2OH$, 56-81-5.

References and Notes

(1) Permanent address: Xerox Research Centre of Canada, 2660 Speakman Drive, Mississauga, Ontario, Canada L5K 2L1.
(2) Permanent address: Department of Chemistry, University of Toronto, Toronto, Ontario, Canada M5S 1A1.
(3) Wirick, M. G.; Waldman, M. H. *J. Appl. Polym. Sci.* **1970**, *14*, 579.
(4) Gray, D. G. *J. Appl. Polym. Sci., Polym. Symp.* **1983**, *37*, 179.
(5) Flory, P. J.; Spurr, O. K.; Carpenter, D. K. *J. Polym. Sci.* **1958**, *28*, 231.
(6) (a) Claesson, S.; Odani, H. *Discuss. Faraday Soc.* **1970**, *49*, 268. (b) Winnik, F. M.; Winnik, M. A.; Tazuke, S. *J. Chem. Phys.*, in press.
(7) (a) Winnik, M. A., Ed. *Photophysical* and *Photochemical Tools in Polymer Science*; D. Reidel: Dodrecht, Holland, **1986**. (b) For another application of pyrene-labeling to study a water-soluble polymer, see: Turro, N. J.; Arora, K. S. *Polymer* **1986**, *27*, 783.
(8) (a) Webowyj, R. S.; Gray, D. G. *Macromolecules* **1984**, *17*, 1512. (b) Nystrom, B.; Bergman, R. *Eur. Polym. J.* **1978**, *14*, 431.
(9) Schnieders, C.; Müllen, K.; Huber, W. *Tetrahedron* **1984**, *40*, 1701.
(10) Best yield and highest purity were obtained when the conditions described in the following reference were observed meticulously: Kabalka, G. W.; Varma, M.; Varma, R. S.; Srivastava, P. C.; Knapp, F. F., Jr. *J. Org. Chem.* **1986**, *51* 2386.
(11) This effect and the observation of other changes in the absorption spectra of fluorescent labels induced by intra- and intermolecular polymer interactions have been reported by Suzuki[12] and by Herkstroeter.[13]
(12) Suzuki, Y.; Tazuke, S. *Macromolecules* **1980**, *13*, 25; **1981**, *14*, 1742.
(13) Herkstroeter, W. G.; Martic, P. A.; Hartman, S. E.; Williams, J. L. R.; Farid, S. *J. Polym. Sci., Polym. Chem. Ed.* **1983**, *21*, 2473.
(14) Roberts, G. A. F.; Thomas, J. M. *Polymer* **1978**, *19*, 459.
(15) Samuels, R. G. *J. Polym. Sci.* **1969**, *7*, 1197.
(16) Nystrom, B.; Roots, J. *Eur. Polym. J.* **1980**, *16*, 201.

Cooperative Binding of Sodium Myristate to Amylose

Paul V. Bulpin, A. Norman Cutler, and Alexander Lips*

Unilever Research, Colworth Laboratory, Sharnbrook, Bedford MK 44 1LQ, U.K.
Received April 25, 1986

ABSTRACT: The binding of sodium myristate to amylose has been studied by a surface tension method. Surface tensions of myristate solutions were compared with those of systems containing amylose. Slow adsorption of amylose–myristate complex at the air–water interface has rendered possible the use of surface tension for estimating mean activities of sodium myristate in the presence of amylose and the construction of a binding isotherm. Information has also been gained on the "surface activity" of complexes. Comparison of the isotherm with optical rotation studies has revealed that a relatively low level of binding can fully induce a conformational transition in the amylose to a helical state. Moreover, this state remains unaffected by the subsequent binding at free myristate approaching the critical micelle concentration. Optical rotation studies together with measurements of surface activity of the complex provide supportive evidence for more than one type of binding process. A cooperative mode of binding is inferred for low free myristate with selective binding to the helical conformer. The cooperative constants and saturation binding for this mode, estimated on linear Ising theory, conform to a model of interrupted but extensive end-to-end packing of extended myristate molecules in the cavity of an amylose helix with six residues per turn. The secondary binding is also cooperative, reflecting lateral hydrophobic attraction between adsorbed myristate molecules and free energies of binding approaching that of micellization.

1. Introduction

Amylose can interact strongly with many polar and nonpolar compounds, including lipids and emulsifiers.[1-5] At the level of secondary structure, the interaction is believed to involve complexed lipid molecules located within single-helical conformations of the amylose. There is strong evidence for this picture from X-ray diffraction studies in the solid state[5-7] and also complementary support from structural studies on aqueous solutions.[8-10]

Research on amylose–lipid interactions has been directed mainly to the structure of the complexes and less to their thermodynamic properties. Differential scanning calorimetry[9,11-13] has been used to characterize the melting of complexes. However, there are only a few quantitative studies on the binding of lipid molecules to the amylose.[14,15] Free energies of amylose–lipid interactions are thus largely uncharacterized, and their full scope may not be fully appreciated.

The subject of this paper is the measurement of binding of sodium myristate to amylose. The conditions chosen closely match those of earlier structural studies[9,10] on the conformational behavior of amylose–myristate systems by optical rotation and NMR methods.

The present objective of complementing studies of secondary structure with thermodynamic measurements has dictated the choice of systems dilute in amylose. Adsorption studies are then not straightforward (in the absence of an established myristate-specific potentiometric method) because of the enhanced difficulty of separating amylose–myristate complex from its surrounding solution and competing adsorption of myristate onto glassware, dialysis tubing, etc. It was found that a surface tension method could be utilized, providing information not only on the binding of myristate to amylose but also on the surface activity of the complexes formed.

2. Experimental Section

Lipid-free amylose (type III, DP = 970) was obtained from Sigma Chemical Co. Ltd. Sodium myristate was prepared from pure myristic acid (BDH) by refluxing with excess sodium hy-

0024-9297/87/2220-0044$01.50/0

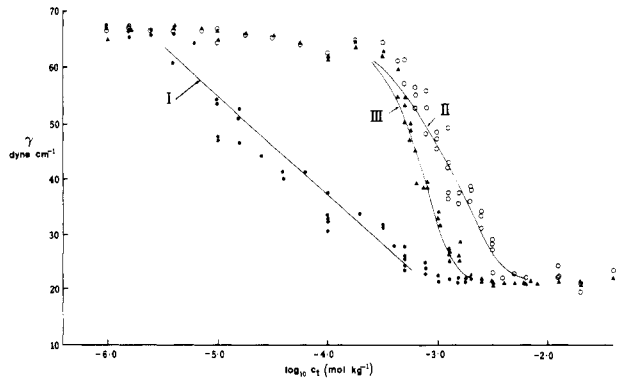

Figure 1. Surface tension of myristate–amylose systems (no added salt, 45 °C, Me_2SO at 2.5% and amylose at 0.1% (w/v)): curve I, myristate in the absence of amylose; curves II and III, myristate in the presence of amylose at 0.1%. Curve II represents initial tensions at ca. 10 s, and curve III equilibrium tensions at long times; full lines are best fits to data according to a Gompertz sigmoidal representation. Abscissa, log c_t (total myristate c_t in units of mol·kg^{-1}); ordinate, γ (surface tension in units of dyn·cm^{-1}).

droxide followed by precipitation in ethanol and repeated washing with ethanol and finally washing with diethyl ether.

Amylose was first dissolved in hot dimethyl sulfoxide (Me_2SO) to give a 4% (w/v) solution and then diluted with boiling water to 0.2% (w/v) amylose and 5% (w/v) Me_2SO. Initial dissolution in the good solvent Me_2SO ensured a reasonably stable, disordered conformational state for the amylose with slow retrogradation kinetics.[16] Sodium myristate solutions were maintained at 45 °C and used within a few hours of preparation. Aliquots of amylose stock were mixed with myristate solutions at 45 °C. All the mixtures had the same concentrations of amylose and Me_2SO, respectively 0.1% and 2.5% (w/v). The measured pH of the mixtures was always greater than 7, typically 8.5, indicating a large excess of myristate over myristic acid and consistent with estimates on the basis of its pK of 4.9.[17] The systems investigated were free of supporting electrolyte.

Optical rotation was measured at 365, 436, 546, and 578 nm on a Perkin-Elmer 241 polarimeter, using 10-cm cells thermostated at 45 °C. The value of specific rotation at the sodium D line was inferred from a standard Drude plot.

For the surface tension studies, a Wilhelmy plate method[18] was utilized. The rectangular plate (0.026 cm wide and 2.5 cm long) was made of stainless steel and was extensively acid washed and rinsed with triple-distilled water prior to use. The plate was immersed to a depth of ca. 1 cm at the air–water interface of amylose–myristate mixtures in a surface tension trough at 45 °C.

A calibration was first established for the dependence of the surface tension of myristate solutions on concentration; this was done in the absence of amylose but in the presence of Me_2SO at a constant level of 2.5% (w/v). Corresponding measurements on myristate solutions in the presence of amylose, at 0.1%, and correspondingly Me_2SO at 2.5%, were then compared with the above calibration for myristate alone. The difference in the two sets of results was interpreted on the basis of binding of the myristate to the amylose. To establish confidence in this procedure it was necessary to investigate the time dependence of the surface tension force acting on the Wilhelmy plate. Amylose–myristate systems were found to display dynamic surface tension effects of unusually slow kinetics, on the scale of minutes to hours, amenable therefore to simple study. The following general procedure was adopted: amylose–myristate mixtures were equilibrated at 45 °C prior to transfer to the surface tension trough at the same temperature, the Wilhelmy plate was immersed as soon as possible after the creation of fresh air–liquid interface, and the changes in surface tension were monitored for ca. 1 h from an initial state of freshly generated surface.

3. Results and Discussion

Figure 1 illustrates the dependence of measured surface tensions on the total concentration of myristate (c_t). For myristate in the absence of amylose (curve I), the slope of the approximately linear part and the myristate concentration at the onset of the lower plateau region are in line with values reported for similar systems,[19] the former indicating a packing density of myristate at the air–water interface of 50–100 Å^2/head group, and the latter a critical micelle concentration (cmc) of $(1.8 \pm 0.3) \times 10^{-3}$ mol·kg^{-1}.

We were unable to detect dynamic surface tension effects for myristate solutions in the absence of amylose (curve I). Even at the lowest levels of myristate, the times for relaxation of dynamic states to the equilibrium tension were less than the measurement time (approximately 10 s), to which we were constrained by the need to achieve stable positioning of the plate in the trough. A pronounced time dependence, on the scale of minutes to hours, could be observed when amylose and myristate were jointly present. This is depicted by curves II and III, the first representing measured "initial" dynamic tensions for freshly generated surfaces, and the second the corresponding "equilibrium" tensions established at long times. Our experience with myristate alone and kinetic studies of dynamic tensions for aqueous surfactant systems[20,21] permit the conclusion that free surfactant monomer, at all the concentrations studied, is fully equilibrated in times less than 10 s. The slow time dependence in the presence of the amylose implicates the biopolymer in a process of slow adsorption at either or both the air–solution and metal plate–solution interface. At both ends of the range of myristate studied, curves II and III concur; this indicates that amylose on its own is only weakly surface active but that binding mediates its surface activity in a manner showing a maximum at an intermediate myristate concentration.

The observed "initial" tensions are intermediate as opposed to pure dynamic tensions[20] and as such might be expected to be difficult to interpret. However, amylose–myristate complex and free myristate achieve interfacial equilibration on widely different time scales. Therefore, the measured initial tensions are reasonably representative of an idealized surface phase that behaves as though it were in equilibrium with only the myristate in the bulk solution and not the polymer; moreover, at the initial stage at ca. 10 s, the concentration of amylose at the surface is very low and its contribution to the dynamic tension can be ignored. Kinetic factors thus create an intermediate but easily measured condition of virtual separation of myristate from amylose. Quantitative support for this conclusion derives from estimates of upper bounds for diffusion rates of myristate and amylose to the interface:[21]

$$t = 6.9 \times 10^{-43} \pi n^2/(c^2 D) \qquad (1)$$

Here, t is the time for adsorption of n molecules per unit area of surface, c is the bulk concentration of the adsorbing molecules, and D is their diffusion coefficient. Reasonable estimates for D are respectively 5×10^{-10} and 3×10^{-11} m^2·s^{-1} for myristate and amylose. To achieve a reciprocal adsorption density of 200 Å^2/molecule (ca. 10 dyn·cm^{-1} change in surface tension) takes ca. 1 ms at the cmc and 10 s at the lowest free myristate studied; for amylose (at 0.1%) the predicted shortest time is of order 10^3 s.

The above establishes confidence in "initial" tensions providing an approximate probe for the mean thermodynamic activity of sodium myristate in bulk solution in the presence of amylose. Moreover, from the comparison between curves I and II we can construct an isotherm for the thermodynamic binding of sodium myristate to the amylose. This is shown in Figure 2, where N represents the adsorption of myristate and c_f is its free equilibrium concentration. In the construction of this isotherm, each set of surface tension data in Figure 1 was first smoothed on the basis of a Gompertz sigmoidal curve fit.

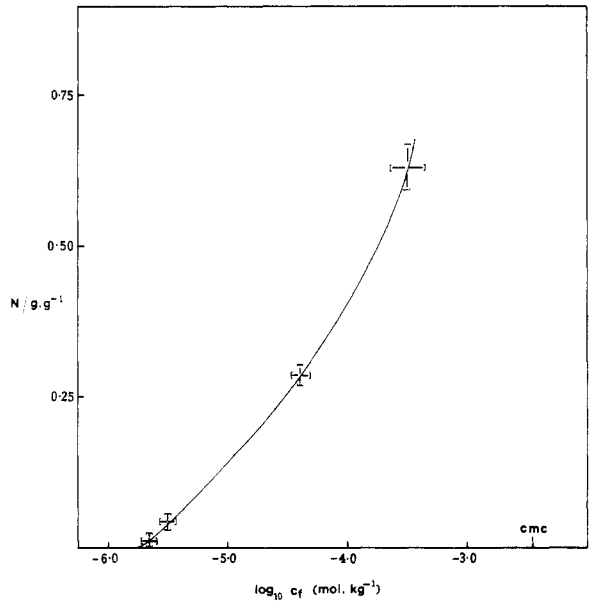

Figure 2. Binding isotherm of myristate to amylose (no added salt, 45 °C, Me_2SO at 2.5% and amylose at 0.1% (w/v)). The isotherm is constructed on the basis of the smoothed curves in Figure 1; error bounds indicated. Abscissa, log c_f (free myristate in units of mol·kg^{-1}); ordinate, N (grams of sodium myristate adsorbed per gram of amylose).

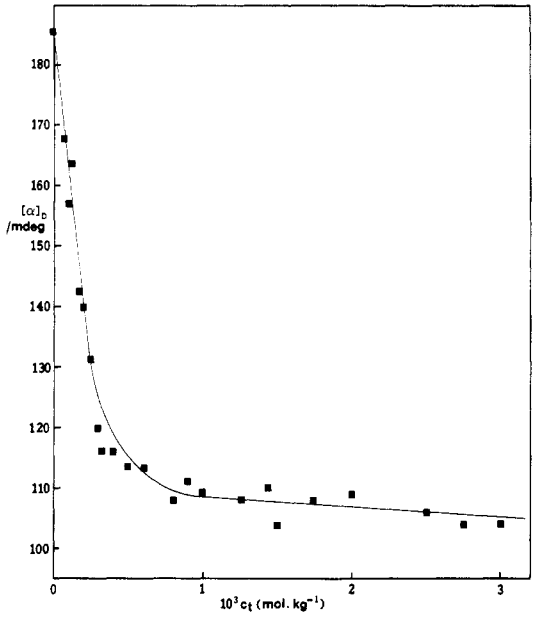

Figure 3. Dependence of optical rotation of amylose on myristate (no added salt, 45 °C, Me_2SO at 2.5% and amylose at 0.1% (w/v)). Abscissa, 10^3c_t (total myristate in units of mol·kg^{-1}); ordinate, $[\alpha]_D$ (specific rotation in mdeg).

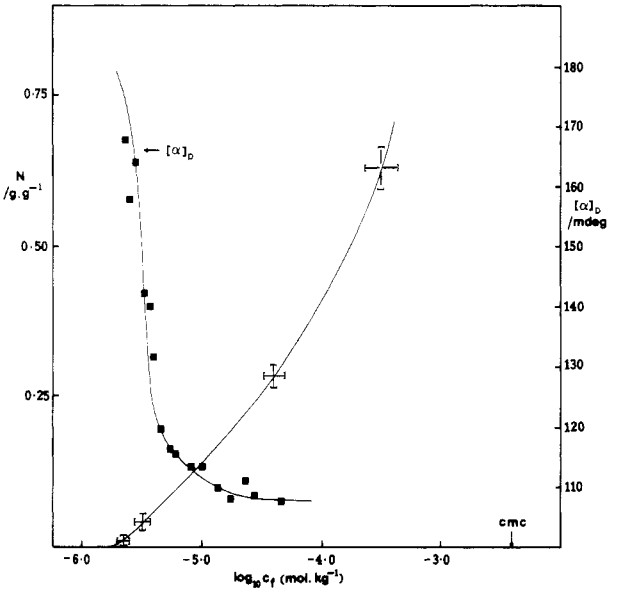

Figure 4. Comparison between binding and optical rotation for amylose–myristate (no added salt, 45 °C, Me_2SO at 2.5% and amylose at 0.1% (w/v)): full line, binding isotherm; data points, measured optical rotations. Abscissa, log c_f (free myristate in unts of mol·kg^{-1}); ordinate (left), N (grams of sodium myristate adsorbed per gram of amylose); ordinate (right), $[\alpha]_D$ (specific rotation in mdeg).

Some further comments on our experimental approach are in order. The sufrace tension force on the Wilhelmy plate varies as $\gamma \cos \theta$, where γ is the surface tension at the air–solution interface and θ is the angle of contact of the test solution on the plate. It was ascertained that myristate solutions fully wetted the plate ($\theta = 0°$) at all concentrations. In the presence of amylose, the plates became hydrophobed on prolonged immersion in the solutions; subsequent wetting with water was not possible even in the case of a large excess of myristate over amylose in the original solutions. Clean plates when dipped through fully aged surfaces immediately experienced a constant surface tension force. In all the systems studied, the magnitude of this force was the same as the equilibrium value for plates that had been in contact with the solution throughout the aging process. The inference is that there can be significant adsorption of complex on the plate and a substantial lowering of its surface energy. However, aging also decreases the air–solution interfacial energy to an extent sufficient to maintain adequate wetting ($\theta = 0°$) of the plate throughout the aging process.

The binding isotherm in Figure 2 indicates cooperativity. Measurements of optical rotary power are shown in Figure 3; the comparison with the isotherm is brought out in Figure 4 and reveals that the change in specific rotation is fully developed at low free myristate far removed from the cmc. One can infer that an initial adsorption step induces a change of secondary structure in the amylose. This change, to presumably a fully developed helical state, requires only a low level of adsorption and is insensitive to subsequent binding.

Our studies of the optical rotary behavior of amylose[22] in the presence of a range of fatty carboxylates (C_{11} to C_{18}) have shown the general behavior of a lower plateau region at high carboxylate, as, for example, in Figure 3. Moreover, the plateau value is independent of chain length.[10,22] This suggests that binding of carboxylate induces a particular conformational change in the amylose; chain length and concentration of adsorbate determine only the extent but not the nature of the transition. The fractional change in optical rotation, $([\alpha_w]_D - [\alpha]_D)/([\alpha_w]_D - [\alpha_p])_D)$, relative to the value in water ($[\alpha_w]_D = 186$ mdeg) and the plateau value at high myristate ($[\alpha_p]_D = 103$ mdeg), is taken as an approximate linear measure of fractional helical content f_H of the chain. An implicit assumption here is the absence of significant helical content in myristate-free amylose. Although it is held that amylose has some pseudohelical character (see ref 16 and references therein), this is likely to be small, particularly at 45 °C. Moreover, such helical features appear inconsequential for optical rotation, unlike the pronounced effects observed for ordered amylose–amphiphile conformations.[9] Comparison with the isotherm, in Figure 5, reveals a region, at low free myristate, over which helical content and adsorption level appear in one-to-one correspondence. This is consistent with the

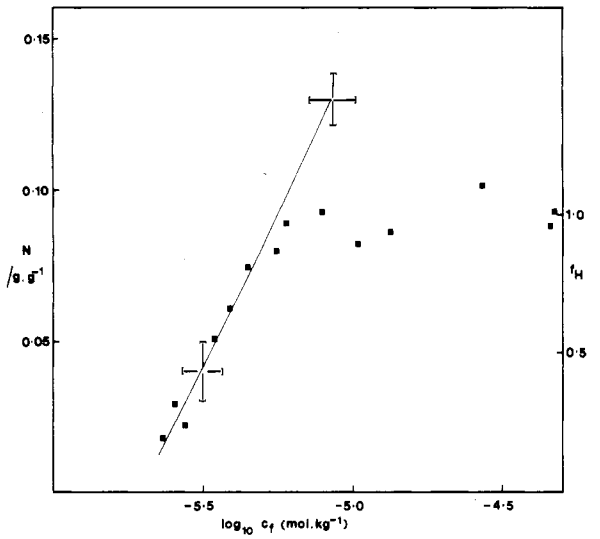

Figure 5. Comparison between binding and development of helix at low free myristate (first binding mode) (no added salt, 45 °C, Me_2SO at 2.5% and amylose at 0.1% (w/v)): full line, binding isotherm; data points, fractional helical content. Abscissa, log c_f (free myristate in units of mol·kg^{-1}); ordinate (left), N (grams of sodium myristate adsorbed per gram of amylose); ordinate (right): $f_H = ([\alpha_w]_D - [\alpha]_D)/([\alpha]_D)/([\alpha_w]_D - [\alpha_p]_D)$ (helical fraction).

reasonable notion that binding takes place only on the helical conformer.[14,23]

Our studies suggest that there are more than one, not necessarily uncoupled binding modes. At low free myristate (helical content $f_H < 0.7$), it is not unreasonable, in view of the observed consistency in structural and adsorption data, to assume that modes other than an initial mode are relatively unimportant. Moreover, the fractional binding saturation β of this mode is expected to equal the inferred fractional helical content of the amylose chain.[14,23] In this case, following general practice,[24-27] we can use a simple linear Ising model; viz.

$$\beta = \tfrac{1}{2}\{1 + (Kuc_f - 1)/[(1 - Kuc_f)^2 + 4Kc_f]^{1/2}\}$$

$$(c_f)_{0.5} = (Ku)^{-1} \qquad (2)$$

$$(d\beta/d \ln c_f)_{0.5} = u^{1/2}/4$$

Here, $(c_f)_{0.5}$ is the concentration of free surfactant at the half-bound point ($\beta = 0.5$). K represents the equilibrium constant for binding to sites whose adjacent sites are free (nucleation step); u is the extent of cooperativitity, i.e., the constant for lateral interaction of occupied sites such that Ku is the binding constant for adsorption to sites adjacent to ones already occupied (growth step). Implicit in the use of eq 2 are the assumptions that interactions are confined to those of nearest neighbors and that the lattice of sites is effectively infinite so that end effects can be ignored. Moreover, the cooperativity is assumed to be dominated by positive contributions from lateral attractive interactions between occupied sites. This permits the concept of an effective site with the condition that each adsorbed molecule can occupy only one such site.[26,27]

The data in Figure 5 for helical content $f_H < 0.7$ was fitted to eq 2. The inferred cooperative parameter $u = 20 \pm 5$. This is similar to that obtained by Yamamoto et al.,[14] for sodium dodecyl sulfate (SDS) adsorbing to amylose. The intrinsic binding constant $K = (1.6 \pm 0.4) \times 10^4$ kg·mol^{-1}, however, is an order of magnitude greater than the corresponding value for SDS. In the potentiometric studies by Yamamoto et al.,[14] attention was focused on conditions of free SDS far removed from the cmc; attempts to fit Scatchard plots to the McGhee and von Hippel

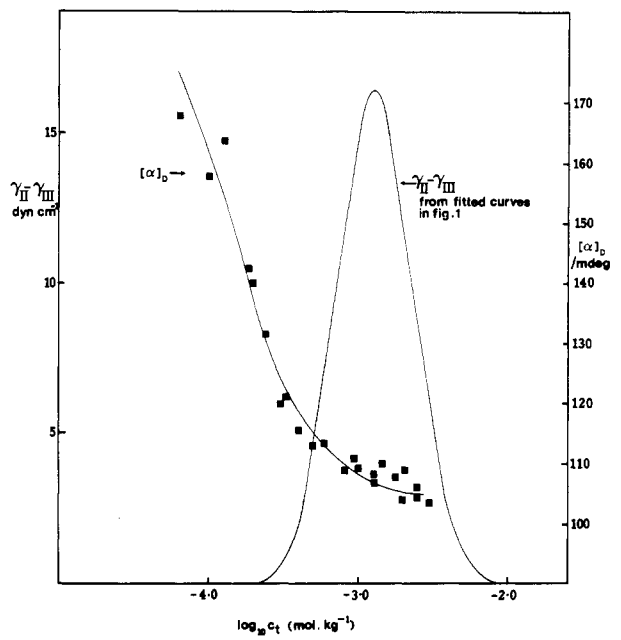

Figure 6. "Surface activity" (from difference between smoothed curves II and III in Figure 1) of amylose–myristate complexes compared with optical rotation behavior (no added salt, 45 °C, Me_2SO at 2.5% and amylose at 0.1% (w/v)). Abscissa, log c_t (total myristate c_t in units of mol·kg^{-1}); ordinate (left), $(\gamma_{II} - \gamma_{III})$ (in units of dyn·cm^{-1}); ordinate (right): $[\alpha]_D$ (specific rotation in mdeg).

model of cooperative, single-mode adsorption[27] proved successful only at low free SDS, and the observed discrepancy between theory and experiment at higher SDS was disregarded on grounds of poor reliability of the measurements. The possibility of additional modes of adsorption was not considered. With myristate, we find clear evidence, independent of adsorption measurements, for at least two types of process. As can be seen in Figure 6, the surface activity of complexed amylose, as represented by the difference between measured initial and final tensions) curves II and III in Figure 1), has a point of inflection and decreases *past* the stage of completion of the conformational transition; the presence of a maximum and the decrease in surface activity at higher myristate approaching the cmc are suggesting secondary interaction of the complex with amphiphile.

It is apparent from Figure 2 that positive cooperativity is a feature also of the binding process near the cmc. This is likely to be due to attractive hydrophobic interactions between bound surfactant molecules. Such behavior is commonly observed[28] and sometimes fitted to models of cooperative binding to a rigid lattice. The linear Ising model for binding to a rigid lattice is mathematically isomorphous with that for a polymer undergoing conformational change as a result of selective binding to one of its conformers. The formalism of eq 2 therefore applies, with u now specifically representing the cooperative constant for lateral aggregation of adsorbed molecules on the lattice. Constancy in optical rotation, observed for $c_f > 3 \times 10^{-5}$ mol·kg^{-1} (Figure 4), justifies the assumption of conformational rigidity in the adsorbent. If we assert that the isotherm can be represented by only two, uncoupled binding modes and fit eq 2 to the region of secondary adsorption near the cmc ($c_f > 5 \times 10^{-4}$ mol·kg^{-1} in Figure 2), we obtain the values $K = (2.1 \pm 0.6) \times 10^2$ mol^{-1}·kg, $Ku = (1.2 \pm 0.2) \times 10^3$ mol^{-1}·kg, and u in the range 4–9. The considerable uncertainty in these estimates reflects the low reliability of measurements close to the cmc; the attempted least-squares fit to a linear Ising model was confined to

data in the narrow range of c_f of 5×10^{-4} to 8×10^{-4} mol·kg^{-1}. On the basis of the shape of the isotherm, this range appears to correspond to a region in the lower half of the cooperative transition, approaching and possibly extending beyond the midpoint. In the absence of data near saturation, the fitted estimate of the position of the midpoint is uncertain, in the range 7×10^{-4} to 1×10^{-3} mol·kg^{-1}. The corresponding estimate of saturation binding of this secondary mode is similarly uncertain, in the range N = 1–2 g·g^{-1}. Despite the poor definition of the isotherm in the cooperative region of the second process, we have attempted the linear Ising representation to provide a convenient, albeit approximate comparison with the first mode. It is relevant here also to note that there are reasons to doubt the adequacy of the uncoupled-two-mode model, which would suggest substantially lower than observed binding for the midrange of myristate concentrations. Improved theoretical representation of the isotherm could derive from inclusion of the concept of positive coupling between the two modes, alternatively and more probably from an allowance for charge effects expressed through variable counterion binding (see later). We have not attempted this for lack of sufficient quality in our data and specific information on counterion binding. Notwithstanding the above reservations, however, our data clearly permit the conclusion that there are at least two modes; both display cooperative features, and their binding constants are widely separated. The first is strongly adsorptive and responsible for changing the conformational state of the amylose. Its state of saturation corresponds to a much lower binding (N = 0.09 g·g^{-1}) than that inferred for the second step (N = 1–2 g·g^{-1}). The standard free energy change of transfer of myristate from the bulk solution to the amylose–myristate environment is given by $-kT$ ln (Ku) and is equal to $-12.7kT$ for the first mode and -7.1 kT for the second. The latter value is close to the inferred standard free energy change for micellization of myristate (kT ln (cmc) = $-6.4kT$), indicating conditions of hydrophobic interaction approaching those in a micellar environment.

It is useful to comment further here on our choice of "initial" rather than "equilibrium" tensions (respectively curves II and III in Figure 1) in the construction of the binding isotherm in Figure 2. Prior to each measurement of tension the amylose–myristate mixtures had been allowed to equilibrate fully; the subsequent time effects in measured surface tensions are associated with the relatively slow transport of complex to the air–water interface. As these effects are completely reproduced in magnitude and time scale whenever a fresh interface is drawn above the preequilibrated solution, the possibility of slow kinetics of complex formation in bulk solution having influenced our measurements can be discounted. Moreover, we were unable to observe time effects in the optical rotation of amylose–myristate mixtures within a time frame of 10 min to 24 h. The preequilibration period in the surface tension studies was typically 8 h. As argued in section 2, the initial tensions represent the adsorption effectively only of the surfactant monomer and therefore directly its thermodynamic activity whereas the equilibrium values reflect the additional presence of complex in the interface and not obviously therefore the monomer activity. Although it is not appropriate therefore to use curve III in the construction of the isotherm, it is worth pointing out that had we done so our conclusions about the first mode would not be significantly affected; moreover, secondary binding would still be indicated but at a lower level in the midrange of free myristate concentrations.

Equation 2 provides a convenient representation of gross features of the binding behavior. Charge effects arising from variable counterion binding[29] or differences in degree of hydrolysis between adsorbed and bulk myristate are implicitly ignored here. The surface tension method purports to provide information equivalent to that of a dialysis experiment, namely the dependence on concentration of the mean thermodynamic activity of the neutral surfactant salt in the presence of the polymer. As described in ref 29 this provides information strictly only on the "thermodynamic binding" of the neutral salt and not specifically of the myristate ion unless assumptions are made about counterion binding. Variation in the latter with extent of binding of the myristate is to be expected. In the region of the first mode, the development of surface charge on the amylose is likely to manifest itself in only minor electrostatic contributions to the interactions of myristate with the polymer and other adsorbed myristate molecules. Then the use of the Ising model with the assumption of effectively zero electrostatic potential of the polymer is probably justified. On the other hand, at high myristate the electric potential of the polymer is likely to be considerable and cannot be neglected. Counterion condensation[29,31] will then be a controlling factor such that the electric potential of the polymer complex is maintained at a high but approximately *constant* value.[31] If this is so, the simple Ising formalism is still applicable but the binding parameters now refer to a nonzero reference potential. It follows that the extrapolation of our Ising representation of binding at high myristate is expected to underestimate the binding in the midrange of the isotherm as the electric potential decreases. This would be consistent with the behavior already noted.

We have not allowed for any specific effects arising from the additional component Me_2SO maintained in all the experiments at constant molality rather than constant chemical potential. Effects due to this were considered slight; the direct contribution of Me_2SO (at 2.5%) to the air–water interfacial tension is less than 0.5 dyn·cm^{-1}.

Complete saturation, β = 1, of the mode responsible for the conformational transition requires a level of adsorption N = 0.09 g·g^{-1}. This corresponds to 0.06 molecule of myristate per anhydrous glucose residue and an average helical length of 22 Å available to each myristate molecule in a helical structure with six residues per turn.[7] The fully extended length of myristate is 20 Å (including the counterion); the optimal length, taking account of end-to-end configurational energy, is ca. 16 Å.[30] It is apparent that the observed behavior would not be not inconsistent with a model of extensive end-to-end packing of extended myristate molecules in the cavity of a sixfold helix. The possibility of helices with more than six residues per turn, binding myristate in less extended configurations, cannot be discounted. However, evidence from X-ray studies and the observed lack of sensitivity of the helical structure to the substantial secondary binding make this less likely. Finally, on the basis of the low cooperativity u = 20 we should expect short helical sequences with frequent interruptions. The average cluster length $\bar{m}$, in units of adsorbed myristate molecules, is given by

$$\bar{m} = 2\beta(u - 1)/\{[4\beta(1 - \beta)(u - 1) + 1]^{1/2} - 1\} \quad (3)$$

At β = 0.5, $\bar{m}$ is ca. 5, corresponding to a helical length of 100 Å. Recent structural studies[7] suggest folding lengths of this order in typical lamellae of packed helices of amylose complexes.

Acknowledgment. We are indebted to Dr. M. J. Gidley from this laboratory and to Prof. D. G. Hall from Unilever

Research, Port Sunlight, England, for helpful discussions.

Registry No. Sodium myristate, 822-12-8; amylose, 9005-82-7.

References and Notes

(1) Bear, R. S. *J. Am. Chem. Soc.* **1944**, *66*, 2122.
(2) French, D.; Pulley, A. O.; Whelan, W. J. *Starke* **1963**, *15*, 349.
(3) Mikus, F. F.; Hixon, R. M.; Rundle, R. E. *J. Am. Chem. Soc.* **1946**, *68*, 1115.
(4) Takeo, K.; Tokomura, A.; Kuge, T. *Starke* **1973**, *25*, 357.
(5) Rundle, R. E.; Edwards, F. C. *J. Am. Chem. Soc.* **1943**, *65*, 2200.
(6) Winter, W. T.; Sarko, A. *Biopolymers* **1974**, *13*, 1461.
(7) Jane, J.-L., Robyt, J. F. *Carbohydr. Res.* **1984**, *132*, 105.
(8) Rees, D. A. *J. Chem. Soc. B* **1970**, 877.
(9) Bulpin, P. V.; Welsh, E. J.; Morris, E. R. *Starke* **1982**, *34*, 1982.
(10) Bulpin, P. V.; Cutler, A. N.; Lips, A. In *Gums, Stabilizers and Thickeners for the Food Industry 3*; Elsevier: Amsterdam, 1986; p 221.
(11) Donovan, J. W.; Mapes, C. J. *Starke* **1980**, *32*, 190.
(12) Kugimiya, M.; Donovan, J. W.; Wong, R. Y. *Starke* **1980**, *32*, 265.
(13) Stute, R.; Konieczny-Janda, G. *Starke* **1983**, *35*, 340.
(14) Yamamoto, M.; Sano, T.; Harada, S.; Yasunaga, T. *Bull. Chem. Soc. Jpn.* **1983**, *56*, 2643.
(15) Yamamoto, M.; Sano, T.; Yasunaga, T. *Bull. Chem. Soc. Jpn.* **1982**, *55*, 1886.
(16) Jordan, R. C.; Brant, D. A. *Macromolecules* **1980**, *13*, 491.
(17) Robb, I. D. *Aust. J. Chem.* **1966**, *19*, 2281.
(18) Padday, J. F. *Surf. Colloid Sci.* **1969**, *1*, 101.
(19) Mukerjee, P.; Mysels, K. J. *Natl. Stand. Ref. Data Ser. (U.S., Natl. Bur. Stand.)* **1971**, *NSRDS–NBS* 36.
(20) Defay, R.; Prigogine, I.; Bellemans, A.; Everett, D. H. *Surface Tension and Adsorption*; Longmans: London, 1966; Chapter XIX.
(21) Davies, J. T.; Rideal, E. K. *Interfacial Phenomena*; Academic: New York, 1963; Chapter 4.
(22) Bulpin, P. V.; Cutler, A. N.; Lips, A., to be published.
(23) Magee, W. S.; Gibbs, J. H.; Zimm, B. H. *Biopolymers* **1963**, *1*, 133.
(24) Satake, I.; Yang, J. T. *Biopolymers* **1976**, *15*, 2263.
(25) Schwarz, G.; *Eur. J. Biochem.* **1970**, *12*, 442.
(26) Schneider, F. W.; Cronan, C. L.; Podder, S. K. *J. Phys. Chem.* **1968**, *72*, 4563.
(27) McGhee, J. D.; von Hippel, P. H. *J. Mol. Biol.* **1974**, *86*, 469.
(28) Hayakawa, K.; Santerre, J. P.; Santerre, J. P.; Kwak, J. C. T. *Macromolecules* **1983**, *16*, 1642.
(29) Hall, D. G. *J. Chem. Soc., Faraday Trans. 1*, **1985**, *81*, 885.
(30) Tanford, C. *J. Phys. Chem.* **1974**, *78*, 2469.
(31) Manning, G. S. *J. Chem. Phys.* **1969**, *51*, 924.

Complex Formation between Copper(II) and Poly(*N*-methacryloyl-L-asparagine)

Abdennbi Lekchiri, Joëlle Morcellet, and Michel Morcellet*

Laboratoire de Chimie Macromoléculaire, UA 351 du CNRS, Université des Sciences et Techniques de Lille Flandres Artois, 59655 Villeneuve d'Ascq Cedex, France.
Received June 30, 1986

ABSTRACT: The complexes formed between copper(II) and a polymeric ligand derived from L-asparagine, poly(*N*-methacryloyl-L-asparagine) (PNMAsn), have been investigated by potentiometric titration, electronic spectroscopy, and circular dichroism. *N*-Isobutyroyl-L-asparagine (NIBAsn) was also synthesized and studied for comparison with its polymeric analogue. It was found that NIBAsn forms only one weak complex with copper(II), with a bonding between the metal and the carboxyl group. With PNMAsn, three complexes have been demonstrated. Some of them involve the deprotonation of the amide group. The difference between the polymeric ligand and the model molecule is discussed in terms of the high local concentration of the ligand and electrostatic interactions.

Introduction

In previous papers[1,2] we have reported the study of copper(II) complexes of an optically active polyacid derived from alanine, poly(*N*-methacryloyl-L-alanine) (PNMA) (I).

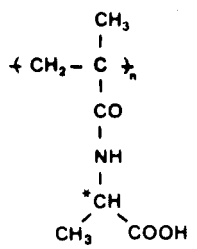

PNMA (I)

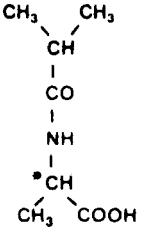

NIBA (II)

The complexing properties of the model molecule of PNMA, *N*-isobutyroyl-L-alanine (NIBA) (II), were also investigated in order to demonstrate the role of the macromolecular chain in the process of complex formation. It was shown that NIBA forms only a weak 1:1 ligand:metal complex through the carboxyl group.

In contrast, PNMA forms a series of different complexes depending on the pH. Some of these complexes involve the deprotonation of the amide group with formation of 1:1 species in one side chain or 2:1 species between two side chains of the polymer (two metal–nitrogen bonds). The present paper reports results obtained in the study of another polyacid derived from an amino acid, poly(*N*-methacryloyl-L-asparagine), with a side chain containing a carboxyl group, a secondary amide, and a primary amide (PNMAsn (III)). PNMAsn has three potential binding sites, and three chelates of different sizes may be formed.

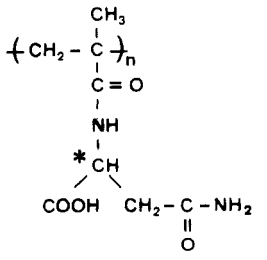

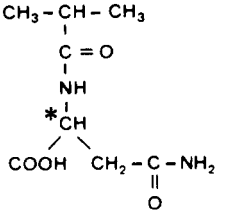

The complexing properties of PNMAsn and its model molecule, *N*-isobutyroyl-L-asparagine (NIBAsn) (IV), have been investigated by potentiometric titration, electronic spectroscopy, and circular dichroism.

Experimental Section

Samples. *N*-Methacryloyl-L-asparagine was prepared from methacryloyl chloride (Fluka) and L-asparagine (Merck) according

0024-9297/87/2220-0049$01.50/0